Available online at www.sciencedirect.com

SciVerse ScienceDirect

Physics Procedia 22 (2011) 549 – 556

Physics Procedia

International Conference on Physics Science and Technology (ICPST 2011)

Geometry Dependent Magnetic Properties of Ni Nanowires Embedded in Self-Assembled Arrays

A.S. Samardak[a*], E.V. Sukovatitsina[a], A.V. Ognev[a], L.A. Chebotkevich[a], R. Mahmoodi[c], M.G. Hosseini[c], S.M. Peighambari[b], F. Nasirpouri[b]

[a]*Laboratory of thin film technologies, School of Natural Sciences, Far Eastern Federal University, 8 Sukhanova str., Vladivostok, 690950, Russia*

[b]*Department of Materials Engineering, Sahand University of Technology, Tabriz 51335-1996, Iran*

[c]*Department of Physical Chemistry, Faculty of Chemistry, University of Tabriz, Tabriz, Iran*

Abstract

Wereporton magnetic properties (coercive force and remanencesquareness) of Ni nanowire arrays embedded in self-assembled alumina templates with pore diameters of 20 and 40 nm. We study magnetic behavior of nanowires both theoretically and experimentally in configurations when an external magnetic field is rotated in-plane and out-of-plane of the sample substrates. Spatial distribution dependent in-plane magnetic anisotropy behavior of the Ni nanowires is explained.

PACS: 75.30 Gw, 75.50. Tt, 75.60.Ej, 75.70.Cn

Keywords: nanowire, alumina template, magnetic anisotropy, coercive force, magnetostatic energy

1. Introduction

Due to the unique properties, magnetic nanowires attract attention of scientists and engineers in last years. The most demanded nanowire applications are high density magnetic storage media [1], GMR sensors [2], biomagnetic [3,4] and medical [5] devices. Fabrication and properties of arrays of magnetic nanostructures are of interest not only from a fundamental but also from a technological point of view [6,7].

*Corresponding author. Tel.: +7-902-489-9292; fax: +7-(432)-243-23-15.
E-mail address: asamardak@gmail.com.

 doi:10.1016/j.phpro.2011.11.085

Highly-ordered nanoporous alumina is a suitable and inexpensive template material for the large scale fabrication of magnetic nanowires arrays. Templating is not an old technique for magnetic media in microscale though interest on this technique is growing rapidly due to the ease of fabrication of materials on the nanoscale range with efficiency and cost effectiveness. There are several ways to fill the nanopores with metals or other materials to form nanowires, but the electrochemical deposition method [8] is a general and versatile method. Various methods are used to prepare nanowires, but the anodic aluminium oxide (AAO) template method [9,10] has been applied widely due to its convenience and inexpensiveness.

Magnetization direction in an individual long wire is defined by the shape anisotropy [11]. In case of a nanowire array, magnetostatic dipole interaction specifies the magnetic behavior of the arrays [12]. Angular dependences of magnetic parameters, such as coercivityH_c and remanencesquarenessSQ can provide helpful information about the rotation mechanisms of magnetic moments not only of individual nanowires, but also of its arrays [12]. However, due to the system complexity of the nanowire array and structural imperfections of nanowires, there are still open questions about the magnetization reversal mechanisms and geometry dependent magnetic properties.

In this paper we present detailed experimental results of angular variation in H_c and SQ for Ni nanowires with diameters of 20 and 40 nm. While magnetic properties, measured when an external magnetic field$\boldsymbol{H}$ is aligned along nanowire long axis$\boldsymbol{L}$, do not depend on diameter and length of nanowires, magnetic behavior at the in-plane configuration ($\boldsymbol{H}\perp\boldsymbol{L}$)is induced by spatial distribution of nanowires in an array. The results discussed in the paper conclude that ferromagnetic nanowires with easy axis of magnetization parallel to the nanowire long axis having the desired values of $H_c$and SQ forperpendicular recording media can be optimized by modifying the spatial order of nanowires in an array.

2. Experimental details

High-purity aluminum foils (99.999%) were anodized after degreasing in acetone for 5 min., chemical surface treatments in KOH 200 g.Lit^{-1}, Na_2CO_3 50 g.Lit^{-1} and HNO_3 50% solutions, and electropolishing under a constant-voltage condition of 16 V for 8 min in a mixture of $HClO_4$: C_2H_5OH (1:4 in vol) at 5^{o}C. Anodization was, then, carried out under a constant cell voltage 40 V in a 0.3 M oxalic acid ($H_2C_2O_4$) and 26 V in a 0.3 M sulfuric acid (H_2SO_4) solutions to obtain nanopore diameter of 40 and 20 nm, respectively. Details of different samples under this study are given in Table 1. The temperature of the electrolyte was maintained at 0-2 ^{o}C during anodization using a cooling system. The solution was stirred vigorously in order to accelerate the dispersion of the heat evolved from aluminum sheets. The formed alumina was then removed by a mixture of 0.3 M chromic acid and 0.5 M phosphoric acid at 60 ^{o}C for an appropriate time depending on the anodizing time. Then, the Al foil was reanodized under the same condition as the first step. For nanowire preparation, thickness of the barrier layer of oxide film was produced in sulfuric acid solution decreased by reducing the anodizing voltage at the end of the second stage of anodizing using 2 V/min steps from 26 V to 20 V, 1 V/min steps from 20 V to 10 V, 0.5 V/min steps from 10 V to 8 V and finally 3 min was kept in 8 V. Then, Ni nanowire arrays were using alternating current electrodeposited into the pores of the alumina templates under 14 or 16V_{rms}, 50 or100 Hz for an appropriate time to precisely fill up the pores(see Table 1). The electrodeposition bath was containing of $NiSO_4.H_2O$ 0.1 M and H_3BO_3 0.5 M with a pH value of solution was adjusted to 3.5.

Table 1.Anodization parameters of alumina templates used for Ni electrodeposition.

Samples	Pore diameter	Nanowire length L	Distance between	Anodizingsolution	Durationofanodization [min]	Depositioncondition

	D [nm]	[um]	wires [nm]			
R2	20	1	60	H_2SO_4	60	$14V_{rms}$, 100Hz
R6	30	2	40	$H_2C_2O_4$	300	$14V_{rms}$, 50Hz
R7	40	2	60	$H_2C_2O_4$	300	$16V_{rms}$, 50Hz

The spatial distribution and dimensional parameters (length and diameter) of the nanowires were studied by high resolution scanning electron microscopy (SEM). SEM images were exploited to process spectral Fourier analysis. Magnetic properties of nanowires were investigated by the home-made vibrating sample magnetometer.For angle variation measurements,the magnetic field was applied at an angle u between the fielddirection and the wire axis. Coercive force $H_c$and remanencesquarenessSQ were derived from themagnetization curves measured at various fixed anglesranged from 0 to 360°.

3. Results and discussion

Magnetic properties of Ni nanowires have strong dependence on diameter, length and spatial distribution in an array. The typical room temperature magnetic hysteresis (M-H) curves for 20 nm (sample R2),30 nm (samples R6) and 40 nm (sample R7) Ni nanowires of length 1 and 2 um, with the external field $\boldsymbol{H}$applied parallel and perpendicular to the nanowire's long axis$\boldsymbol{L}$, are shown in Figure 1. The difference between the perpendicular and parallel M-H curves defines the uniaxial anisotropy for Ni nanowire arrays. In case of $\boldsymbol{H} \parallel \boldsymbol{L}$the remanencesquareness$SQ = M_r/M_s$, where M_r is remanent magnetization and M_s is saturation magnetization, was about 0.9 for all samples. When $\boldsymbol{H} \perp \boldsymbol{L}$we measured very narrow hysteresis loops with small SQ. It means that the easy axis of magnetic anisotropy favors theparalleldirection to the nanowire axis. The coercive force and saturation magnetization for the nanowires with a diameter of 20 nm is higher than for those with bigger diameter. This is the result of an influence of structural imperfections on magnetic behavior of nanowires.

There are two basic mechanisms of magnetization reversal: coherent rotation and curling of magnetization (non-coherent rotation). The value of SQ for all samples is near 100% that considers single domain structure and homogeneous rotation of magnetization in nanowires [13]. As shown in Ref. [14]for magnetic nanowires the magnetization reversal mechanismdepends upon its diameter. Inmagnetic materials the critical diameter forthe transition from coherent rotation to the curling of magnetization is given by follows[15]:

$$D_c = 2.08\ (A^{1/2}/\ M_s), \tag{1}$$

where$A$ is the exchange constant.For Ni nanowires with $A=9\times10^{-7}$ erg/cm, M_s=484 emu/cm^3 we found D_c=41 nm. As diameters of our samples $D < D_c$, the main magnetization reversal mechanism is coherent rotation of magnetization in nanowires. However, Eq.1 is correct for a single wire only and does not include the magnetostatic dipole interaction of wires in an array and structural defects of nanowires.

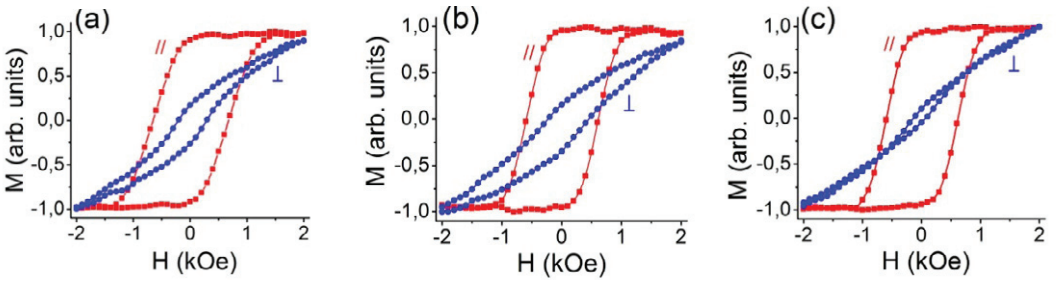

Fig.1. M-H curves for Ni nanowire arrays: (a) R2, (b) R6 and (c) R7. The magnetic field is aligned parallel to nanowire long axis $\boldsymbol{H} \parallel \boldsymbol{L}$and perpendicular to it$\boldsymbol{H} \perp \boldsymbol{L}$.

For nanowire application as a perpendicular recording media the effective anisotropic field H_k plays the main role. There are three basic contributions into H_k: (1) the field of shape anisotropy, which induces a magnetic easy axis parallel to the nanowire's long axis; (2) the field of magnetostatic interaction between nanowires in an array, which tries to rotate the easy axis perpendicular to the nanowires; (3) the magnetocrystalline anisotropy field H_k. The effective anisotropic field H_{eff} can be defined as follows [12]:

$$H_{eff} = 2\pi M_s - 6.3\pi M_s r^2 L / D^3 + H_k, \quad (2)$$

where$r$ is the radius of the nanowire, L is the length and D is the interwire distance. The second term in Eq.2 is the total magnetostatic field acting on one wire. If the magnetostatic field is equal to the sum of the shape anisotropy field and the magnetocrystalline field, than H_k is zero. It means that we can manipulate the value of H_k if L is changed. From Eq.2we can define a critical nanowire length, below which the easy axis is aligned perpendicular to the nanowire long axis:

$$L = L_c = 2D^3 / 6.3r^2 \quad (3)$$

We defined value of L_c as 685, 90 and 171 nm for R2, R6 and R7 samples, respectively. All the values are less thanthe actual length of the nanowires. Below L_c nanowires have an in-plane magnetic anisotropy.

To carry out a detail study of magnetic behaviour of Ni nanowires we measured angular dependences of coercive force $H_c = f(\theta_H)$ and remanencesquareness SQ = $f(\theta_H)$. Results for samples R2, R6 and R7 are shown in Fig.2. All polar diagrams $H_c = f(\theta_H)$look the same for different samples. It manifests that coercivity$H_c$measured at configuration $\boldsymbol{H} \parallel \boldsymbol{L}$ does not depend on diameter and length of nanowires and has the same value H_c = 600 Oewhich is actually much smaller than$2\pi M_s$=3045 Oepredicted for individual wires.The probable mechanism of magnetization reversal is non-coherent rotation so called curling of magnetization [17]. Our resultssuggest that the magnetostaticdipole coupling between nanowires and magnetocrystalline anisotropy cannot be neglected. At this case $SQ \approx 0.95$, which means that the easy axis of magnetization lies along nanowires, while the hard axis is aligned perpendicular them. The bell-shaped behavior of SQ on θ_H is the proof of curling of magnetization in nanowires [12].

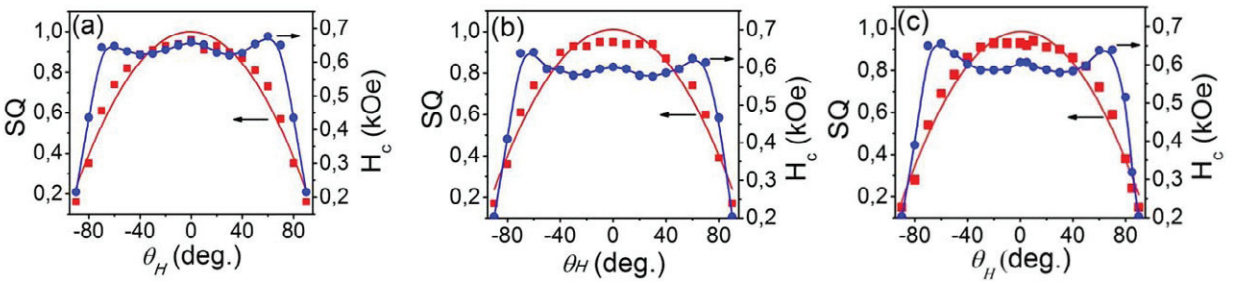

Fig.2. Angular dependencesof coercivity$H_c = f(\theta_H)$ (*a,c,e*) andremanencesquareness$SQ=f(\theta_H)$*(b,d,f)* of Ni nanowire arrays: (*a,b)* – sample *R2*; (c,d) – sample *R6*; (e,f) – sample *R7*. $\theta_H$is the angle between the magnetic field directionand the long axis of nanowire.

The energy of uniaxial magnetic anisotropy of nanowires in case $\boldsymbol{H} \parallel \boldsymbol{L}$ can be defined as $K_u = \Delta N M_s^2 = 7.8\times10^5$ erg/cm^3, where $\Delta N = N_D - N_L = 2\pi$ (N_D and N_L are the demagnetizing factors perpendicular and parallel to the nanowire long axis).Incompliancewiththetheory [16] the coercive force of a polycrystalline nanowire can be calculated as a sum of components caused by the dispersion of crystallographic anisotropy axes H_{CK} and the structural defectsH_{CM}:

$$H_{CK} = \frac{K_1}{2M_s}\sqrt{3{,}23\,\frac{a}{\delta_\omega}\ln\left(\frac{L}{\delta_\omega}\sqrt{3}\right)}, \quad (4)$$

whereK_1=5.7×10^4 erg/cm^3 is the crystallographic anisotropy constant, a is a grain size,

$\delta_w = \pi\sqrt{\left(\frac{2A}{K_{MS}+K_1}\right)}$ = 47 nm is a domain wall width, A=0.9×10^{-6} erg/cm is an exchange constant, K_{MS}=7.39×10^{5}erg/cm^3, and

$$H_{CM} = 17.6\,M_s\,\frac{V_d}{\delta_w^3}\sqrt{\frac{\delta_w}{a}\,ln\,\frac{L}{\delta_w}}, \quad (5)$$

whereV_d=2.19×10^{-18} cm^3 is the volume of structural defect with radius 5.5 nm, L=1 um. As a result, we defined that H_{CK}=130.73 Oe and H_{CM}= 482.24 Oe. Coercivity is the sum of $H_c = H_{CK} + H_{CM}$= 612.97 Oe, which is matching with the experimental value ~ 630 Oe.

To study geometry dependent magnetism of Ni nanowire arrays we plotted the polar diagrams on magnetic parameters of Ni nanowires for case when $\boldsymbol{H}\perp\boldsymbol{L}$and rotated in the sample plane, Fig.3. The angular dependences $H_c = f(\theta_H)$ are the same as for $M_r/M_s = f(\theta_H)$. Maximum values of H_c and M_r/M_smeasured at in-plane configuration were ~ 300 Oe and 0.25, correspondingly. The represented diagrams show that in spite of the M_r/M_s(*SQ*) value, measured at $\boldsymbol{H}\perp\boldsymbol{L}$configuration, significantly less than for latter taken at $\boldsymbol{H} \parallel \boldsymbol{L}$configuration, the in-plane anisotropy has preferential directions of magnetization. Sample R2 has three preferential directions of magnetization(six-fold magnetic anisotropy) matching the hexagonallattice of the alumina templateFig.3(a,b). The imperfection in spatial distribution leads to another behavior of in-plane magnetic anisotropy as shown in Fig.3(c-f): two (c,d) and four (e,f) fold magnetic anisotropy.

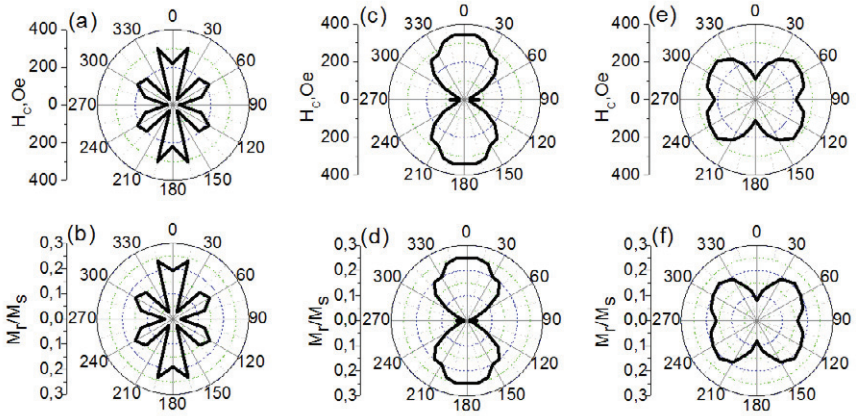

Fig.3.Angular dependences of $H_c = f(\theta_H)$ (*a,c,e*) and $M_r/M_s = f(\theta_H)$ *(b,d,f)* of Ni nanowire arrays: (*a,b)* – sample *R2*; (c,d) – sample *R6*; (e,f) – sample *R7*. An external magnetic field is alignedperpendicular to the long axis of nanowires and rotated in the sample plane.

To explain the difference in behavior of in-plane magnetic anisotropy, we acquired two-dimensional Fourier spectra using SEM images of spatial distribution of nanoporesin the alumina templates, Fig.4. As shown in the SEM images, samples have near hexagonal distribution of nanopores filled by Ni. There are three obvious directionsin Fourier spectra (Fig.4(a)) due to long-range order of nanopores in sample R2. However, for samples R6 and R7 there is no long-range order in nanopore spatial distribution. In Fig.4(b) only one preferential direction of magnetization can be observed, while in Fig.4(c) – two only. Fourier spectra are in a good agreement with the polar diagrams presented in Fig.3. This proves that the behavior of in-plane magnetic properties is defined by the spatial distributionof Ni nanowires.

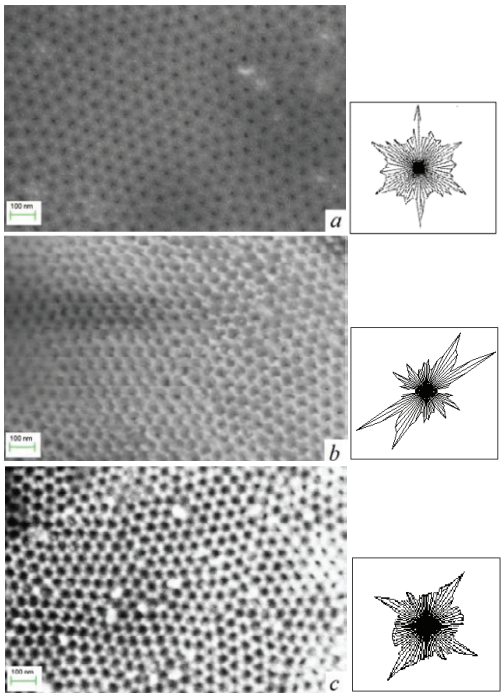

Fig.4.SEM images of nanopore spatial distribution (left) and Fourier spectra (right), acquired from these images, for samples *R2* (a), *R6* (b) and *R7* (c).

4. Conclusions

We carried out the experimental investigation of coercivity and squareness of Ni nanowire arrays in cases of parallel and perpendicular magnetic field orientation relative to the nanowire long axis. All arrays with different geometrical parameters have perpendicular anisotropy oriented with a small angle to the normal of sample plane. This tilt in direction of perpendicular anisotropy is the reason in an existence of in-plane anisotropy component specified by spatial distribution of nanowires. Theoretical estimations of coercivity were done including interwiremagnetostatic interaction and structural imperfections. It helped to conclude of curling of magnetization reversal mechanism in nanowires even with smalldiameter 20 nm.

The results discussed herereveal that ferromagnetic nanowires with easy axis of magnetization parallel to the wire's long axis having the desired magnetic properties forperpendicular recording media and spintronic application can be obtained by modifying the spatial geometry of nanopores in alumina templates.

Acknowledgments

TheresearchissupportedbyFCP "Cadres" under contracts 16.740.11.0502 and 02.740.11.0549, and by the President of Russia's grant MK-5181.2011.2.

References

[1] Albrecht M., Moser A,Rettner CT, Anders S, Thomson T, TerrisBD. (2002). Writing of high-density patterned perpendicular media with a conventional longitudinal recording head. *Appl.Phys. Lett.*2002; **80**: 3409-3413.

[2] Nasirpouri F, Southern P, Ghorbani M, AIrajiZad, Schwarzacher W. GMR in multilayered nanowires electrodeposited in track-etched polyester and polycarbonate membranes. *JMMM* 2007; **308**: 35-39.

[3] Hultgren, A,Tanase M, Chen CS, Meyer GJ, Reich DH.Cell manipulation using magnetic nanowires.*J. Appl. Phys.*2003;**93**: 7554 – 7556.[4] Reich DH,Tanase M, Hultgren A, Bauer LA, Chen CS, Meyer GJ. Biological applications of multifunctional magnetic nanowires.*J. Appl. Phys.*2003;**93**: 7275–7280.

[5] McGary PD, Tan L,Zou J, Stadler B, Downey PR, Flatau AB. Magnetic nanowires for acoustic sensors. *J. Appl. Phys.* 2006; **99**: 08B310.

[6] Kashi MA, Ramazani A,Khayyatian A. The influence of the ac electrodeposition conditions on the magnetic properties and microstructure of Co nanowire arrays.*J. Phys. D: Appl. Phys.*2006; **39**: 4130–4135.

[7] Pirota KR, Navas D, Hernández-Vélez M, Nielsch K, Vázquez M. Novel magnetic materials prepared by electrodeposition techniques: arrays of nanowires and multi-layered microwires. J. Alloys and Compounds 2004; **369**: 18–26.

[8] Nasirpouri F.New Developments in Electrodeposition and Pitting Research.A. El Nemr, Ed. India: Research Signpost Publication, 2007,pp. 55–92.

[9] Li WX, Zhang J, Shen TH, Jones G, Grundy PJ. Magnetic nanowires fabricated by anodic aluminum oxide template—a brief review.*Sci China PhysMech Astron*. 2011;**54**: 1181–1189.

[10] Sarkar J, Gobinda GK,Basumallick A. Nanowires: properties, applications and synthesis via porous anodic aluminium oxide template. *Bull. Mater.Sci.* 2007; **30**: 271–290.

[11] Metzger RM, Konovalov VV, Sun M, Xu T, Zangari G, Xu B, Benakli M, Doyle WD.Magnetic Nanowires in Hexagonally Ordered Poresof Alumina. IEEE Trans. Magn. 2000; **36**: 30-35.

[12] Han GC, Zong BY, Luo P, Wu YH.Angular dependence of the coercivity and remanence of ferromagneticnanowire arrays.*J. Appl. Phys.* 2003; **93**: 9202-9207.

[13] Nielsch K, Wehrspohn RB, Barthel J, Kirschner J, Gosele U, Fischer SF, Kronmuller H. Hexagonally ordered 100 nm period nickel nanowire arrays.*J. Appl. Phys.* 2001; 79: 9202-9207.

[14] Zeng H, Skomski R, Menon L, Liu Y, Bandyopadhyay S, Sellmyer DJ.Structure and magnetic properties of ferromagnetic nanowires in self-assembled arrays.*Phys. Rev. B* 2002;**65**: 134426.

[15] Aharoni A,Shtrikman S.Magnetization curve of the infinite cylinder.*Phys. Rev.*1958; **109**: 1522.

[16] Ivanov AA, Orlov VA. Comparative analysis of domain wall pinning mechanisms in a nanowire.*FizikaTverdogoTela* 2011; **53**: 2318-2326 (in Russian).

[17] SattlerKD.Nanotubes and Nanowires.CRC Press 2010, 784p.